SYNTHESIS AND STRUCTURAL ANALYSIS OF SOL GEL DERIVED STOICHIOMETRIC MONOPHASIC HYDROXYAPATITE

ANBALAGAN BALAMURUGAN, JEAN MICHEL, JOËL FAURÉ, HICHAM BENHAYOUNE, LAURENCE WORTHAM, GANESH SOCKALINGUM*, VINCENT BANCHET**, SYLVIE BOUTHORS, DOMINIQUE LAURENT-MAQUIN*, GÉRARD BALOSSIER

INSERM ERM 0203, Laboratoire de Microscopie Electronique Analytique, Université de Reims, 21, Rue Clément Ader, 51685 Reims Cedex 2, France
**Unité MéDIAN, CNRS UMR 6142, UFR de Pharmacie, Université de Reims,51, rue Cognacq-Jay, 51096 Reims cedex, France*
***Laboratoire de Tribologie et de Dynamique des Surfaces (LTDS), UMR CNRS 5513, Ecole Centrale de Lyon, département STMS, 36 avenue Guy de Collongue, 69134 Ecully, France*

E-mail: gerard.balossier@univ-reims.fr

Submitted July 14, 2005 ; accepted November 25, 2005

Keywords: Sol-gel, Monophasic, Hydroxyapatite (HAP), Biocompatible, Biomaterial

This paper reports on a novel sol-gel technique for synthesis phase pure hydroxyapatite $Ca_{10}(PO_4)_6(OH)_2$ powder. Triethyl phosphite and calcium nitrate were used as phosphorus and calcium precursors, when the stoichiometric Ca/P ratio 1.67 was maintained. The powders obtained were dried and calcined at different temperatures up to 900°C. X-ray diffraction analysis and Raman spectra showed the presence of phase pure HAP. The powders exhibited the FT-IR signature peaks of HAP. In addition, morphological characterizations of the HAP powder was carried out using STEM, EDXS and EELS. The STEM micrographs indicated mill-fractured surface of a HAP particles. The elemental composition analyzed by EDXS and EELS showed the powder calcined at 900°C contains monophasic stoichiometric HAP.

INTRODUCTION

Hydroxyapatite (HAP) ceramics belongs to a class of calcium phosphate-based biomaterial, which has been widely used as bone substitute for long time. In recent years, synthetic HAP has assumed substantial interest and importance due to its chemical similarity with the natural Ca phosphate mineral present in a biological hard tissue. Considering the wide applications of calcium phosphate compounds in biomedical fields, numerous HAP synthesis techniques have been developed. The most commonly used technique for the preparation of HAP is the precipitation technique, involving wet chemical reactions between the calcium and phosphate reagents under controlled temperature and pH conditions [1 5]. However, this method has some inherent disadvantages, primarily the difficult control of the pH value over 9 to avoid the formation of a Ca-deficient HAP which on sintering undergoes easy decomposition, forming tricalcium phosphates.

In this respect, the sol-gel technique is an effective method for the preparation of monophasic powder due to the possibility of a strict control of the process parameters. This method offers a molecular mixing of the calcium and phosphorus which is capable of improving the chemical homogeneity. The sol-gel product characterized by nano-size dimension is an very important parameter to improve the contact and stability at the artificial/natural bone interface.

Moreover, the high reactivity of the sol-gel powder allows a reduction of the processing temperature and degradation phenomena occurring during sintering. The major limitation of the sol-gel technique is linked to the possible hydrolysis of phosphates [6]. Hence, the present investigation proposes a new method to prepare a phase pure HAP powder via the sol-gel route.

EXPERIMENTAL

Triethyl phosphite (Sigma, UK) sol was diluted in anhydrous ethanol and then a small amount of distilled water was added for hydrolysis. The molar ratio of water to the phosphorus precursor is kept at 3. The mixture was sealed in a glass beaker immediately after solvent addition then stirred vigorously. Due to the immiscibility between the phosphite and water, the mixture initially appears opaque, light being scattered by the emulsion phase. However, after approximately 30 min of mixing the emulsion transformed into a clear solution suggesting that the phosphite was completely hydrolyzed. This was confirmed by the loss of phosphite odour of the mixture. A stoichiometric amount (i.e. to maintain Ca/P = 1.67) of 3M calcium nitrate (Aldrich, UK) dissolved in anhydrous ethanol, was subsequently added dropwise into the hydrolyzed phosphorus sol. Vigorous stirring was continued for an additional 10 min after the titration. As a result of this process, a clear solution was

obtained and aged at room temperature for 16 h before drying. The solvents were then driven off at 60°C until a viscous liquid was obtained. Further drying of the viscous liquid at 60°C resulted in a white gel. The gel was ground with a mortar and pestle into fine powder and subjected to different calcination temperatures, from 300 to 900°C with 25-50°C intervals, for 2 h.

FT-IR analysis

The functional group analysis was performed by Fourier Transform Infrared Spectroscopy (FT-IR). The measurements were carried out in the transmission mode in the mid-infrared range (400-4000 cm^{-1}) at the resolution of 4 cm^{-1}. The studies were performed using the FT-IR, Spot light 300, Imaging system, Perkin-Elmer, France. For FT-IR measurements, KBr pellets containing the exactly weighted amount of the substance examined were prepared.

Raman micro spectroscopic assessment

In the laser Raman micro spectroscopy, a continuous laser beam is micro focused on the sample through a microscope. The photons interact with the molecules of the sample by the phenomenon of Raman scattering, an inelastic light scattering process in which a small amount of energy is removed from the laser photon and is transferred to a molecular vibration. Crystallographic characteristics of the mineral crystals can be obtained from wavenumbers and bandwidths of peaks in the recorded spectrum. Confocal Raman microscope (LabRam, Horiba, Jobin-Yvon, France) consisting a point-focus ≈ 785 nm He-Ne laser source, a microscope (Olympus BX41) and a stigmatic spectrometer was used. The sample was placed on the stage of the microscope using a custom-made fixture such that the sample thickness was oriented perpendicularly to the laser beam incident from a 50× microscope objective. Four spectra in the range 400-1200 cm^{-1} were captured across the thickness of the gel to verify that the mineral growth was not limited to surface alone but also included the diffusion of calcium and phosphate ions into the bulk of the gel. Locations of interest were positioned with a motorized *x–y* stage and an optical camera. Each point scan lasted 180 s and the average of three consecutive scans was taken to obtain the final spectrum at a given location. An 1800 g/mm grating provided a spectral dispersion of about 1 cm^{-1}/pixel. The data were acquired using the Labspec software (Jobin Yvon Horiba, France). The crystallinity of the mineral phase was calculated as the inverse of the bandwidth at half the maximum intensity of the symmetric phosphate stretch band. A greater crystallinity factor indicates larger crystals and/or stoichiometrically more ordered composition.

X-ray diffraction analysis

Crystalline phases of calcined powder were investigated using X-ray powder diffraction method (Rigaku D/max-IIB). X-ray radiation of Cu Kα (λ = 1.5418 Å) is set at 30 kV and 20 mA. Identification of crystalline phases was done by comparing with JCPDS files.

Specimen preparation for STEM and X-ray microanalysis

The hydroxyapatite powder was embedded in resin (AGAR, Essex, England). Thin sections of 100 nm nominal thickness were prepared by means of a FC 4E Reichert Young ultramicrotome. The sections were placed on a copper grid (200 Mesh). Sections were coated with a conductive layer of carbon in a sputter-coater to avoid charging effects. The sections were studied with a scanning transmission electron microscope (Philips CM30) operating at a voltage of 100 kV. The microscope is fitted with an energy dispersive X-ray spectrometer (EDXS 30 mm^2 Si(Li) R-SUTW detector) and a parallel electron energy-loss spectrometer (Gathan model Enfina) placed under the STEM colum. Analyses are carried out using a beryllium specimen holder with a 30° tilt. The electron probe diameter is ~13 nm. The EDXS spectra are acquired at an accelerating voltage of 100 kV, with an energy resolution of 10 eV per channel and an electron dose of ~ 3 10^6 nm^{-2}. The EELs experiments were performed at an accelerating voltage of 250 kV with an energy dispersion of 0.1 eV per channel. Elemental profiles from the centre to the periphery of the particles were performed using energy dispersive X-ray spectrometry. The concentration profiles were made across three different particles. The elemental composition was determined by using the Cliff and Lorimer method [7] and [8].

RESULTS AND DISCUSSION

Charecterisation of the gel

Initial preparation of the sol, pH = 2.85 was identified as appropriate pH for this ethanol-based sol preparation and the pH was constant for 48 hrs. In anhydrous ethanol, alkyl groups may form $Ca(OR)_y(NO_3)_{2-y}$ and replace some of the nitrate groups. It is interesting to note that both the translucent gel and the viscous sol, showed a reversible and reproducible flow behavior, i.e. from low viscosity on heating to high viscosity on cooling. However, the viscous sol could be re-dissolved into the solvent to form a clear sol solution as initially prepared, whereas the translucent suspension was observed when the translucent gel was "re-dispersed" in the solvent. This suggests that the colloidal particles (which are large enough to scatter incident visible light) once

developed can hardly be dispersed due to strong interparticle bonding. Although the bonding nature is unknown, this observation suggests a particulate nature of the resulting sol. According to the study of Gross et al. [9], the polymerization of the phosphite cannot proceed indefinitely. Instead, it will be limited to a certain degree of polymerization due to progressively weakly charged hydroxyl ligands. The polymerization stops when the partial charge of the hydroxyl groups approaches zero or positive charge, according to the partial charge model proposed by Livage et al. [10]. The colloidal particles can thus be considered as an aggregation of oligomeric particles. Extended heating of the viscous sol at 60°C resulted in a white solid gel. Upon ageing, the hydrolyzed phosphorus sol (which may be in the form of phosphoric acid ester, $PHO(OEt)_2$, or more generally, $P(OEt)_{3-x}(OH)_x$) interacted with Ca sol, possibly in the form of $Ca(OEt)_y(NO_3)_{2-y}$ in anhydrous ethanol and Ca^{2+} in water, to form oligomeric derivatives containing Ca–O–P bonds. For the ethanol-based process, the reaction may proceed as follows:

$$P(OEt)_{3-x}(OH)_x + Ca(NO_3)_{2-y}(OEt)_y \rightarrow (OEt)_{y'}(NO_3)_{2-y'}- \\ -Ca-O-HPO(OEt)_{3-x'} + H_2O + C_2H_5OH \quad (1)$$

Reaction (1) is rather simplified and idealized chemical form for ethanol medium. Although not strictly precise, they offer some understanding on phase formation based on forthcoming analysis. Further heating of the gel causes removal of the solvents, accompanied by accelerated thermal dehydration or polymerization/condensation between these derivative units, resulting in the formation of more (–Ca–O–P–) containing bonds in the dry gels.

The first stage after making the sol is gelation, where sufficient polymerization has occurred to form a cross-linking of the molecules making up the skeletal structure. The next stage is ageing. The third stage is drying, during which excess solvent is removed. The final stage is sintering, during which the porous structure is eliminated, the residual organisms are removed, and the minerals are crystallized. Especially noticing the ageing stage, the resulting cross-linked structure of the molecules would increase during ageing. As the ageing time increases, the cross-linked structure also increases. According to the results of this study, it seems reasonable to assume that the larger the cross-linked structure, the larger the final HAP powder.

FT-IR analysis

The FT-IR spectrum of the HAP powder is shown in figure 1. There is a broad envelope between 3800 and 2600 cm^{-1} due to the O–H stretch of water and HAP. The O–H groups are hydrogen bonded. The sharp peak at 3566 cm^{-1} is assigned to unhydrogen bonded free O–H stretch which may be present at the surface of the crystallites. The peak at 1636 cm^{-1} is assigned to bending mode of water. The intense broad peak between 900 and 1100 cm^{-1} is assigned to PO_4^{3-}. The stretching and the bending modes of PO_4^{3-} appeared at 602 and 562 cm^{-1} as intense sharp peaks. van der Houwen et al. reported identification of HPO_4^{2-} based on its water absorption bands at 1210 cm^{-1} together with one at 1130 cm^{-1} (shoulder to the absorption band at 1099 cm^{-1}) and a clear absorption band at 879 cm^{-1}. But these features are not clearly evident in the spectrum, as the absorption band due to PO_4^{3-} of HAP is intense and broad. But the distinct shoulder at 868 cm^{-1} indicates the presence of HPO_4^{2-} in the structures. van der Houwen et al. reported dissolving of atmospheric CO_2 yielding CO_3^{2-} based on the peaks at 1456 and 873 cm^{-1} as the process was carried out in alkaline range (pH = 10.5) [11]. Since the present synthesis was also carried out in the alkaline range similar process should also occur. But in the FT-IR spectrum, there is no sharp peak at 1456 and 873 cm^{-1}. But a close observation of the spectrum shows a shoulder at about 1456 cm^{-1} in the spectrum of the as-prepared material. But there are no separate patterns for $CaCO_3$ in XRD patterns of the as prepared HAP. Hence it could be expected to be present in traces in the sample. The peaks at 624 and 3566 cm^{-1} are assigned to OH group of HAP. Theoretically, there are four vibrational modes present for phosphate ion ν_1, ν_2, ν_3 and ν_4 all the four modes are IR active and are observed in HAP spectra. The ν_1 and ν_3 phosphate bands in the region of 900-1200 cm^{-1} and ν_4 absorption bands in the region of 500-700 cm^{-1} are used to characterize apatite structure. The spectral bands in the range 900-1200 cm^{-1} containing symmetric ν_1 and asymmetric ν_3, P–O stretching modes of the phosphate groups were observed. The symmetric P–O stretching mode for HAP occurs at 962 cm^{-1}, which indicates typical HAP structure. The peaks at 630 and 3570 cm^{-1} are the characteristic peaks for stoichiometric HAP [12]. It should be noted that absorption bands at 3581, 3561, 3487, 3320, 2430, 1283 and

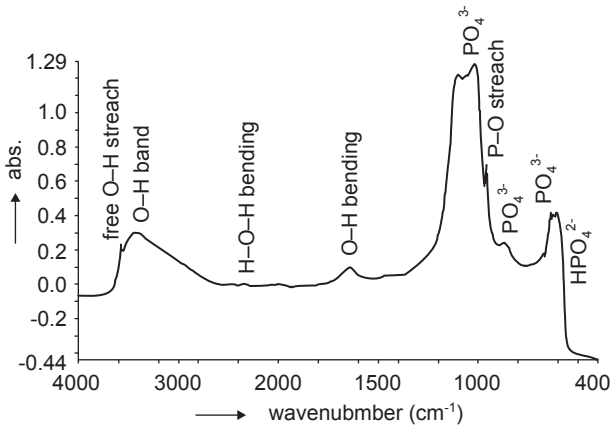

Figure 1. FT-IR spectrum of the monophasic hydroxyapatite.

917 cm^{-1}, which distinguish the formation of octacalcium phosphate are absent and that confirm the HAP stoichiometry. The characteristic peaks for -TCP reported at 950 and 975 cm^{-1} were also absent in the stoichiometric (Ca/P ratio = 1.67) HAP.

Raman spectroscopic analysis

A typical Raman spectrum of a mineralized gel is shown in figure 2. The spectrum for HAP shows four distinguishable groups of spectral bands the first group consists of two bands at ~ 432 and ~ 442 cm^{-1}. These bands correspond to the factor group splitting of the ν_2 bending vibrations of the PO_4^{3-} ion. The bands present at ~ 579, 592 and 608 cm^{-1} belong to the ν_4 fundamental vibrational mode and arise from the triply degenerate bending vibrations. The phosphate symmetric-stretch peak was observed in the range of 962 cm^{-1} which is characteristic for hydroxyapatite [13]. An increasing wave number for this peak indicates a more crystalline stoichiometry of hydroxyapatite particles. The very intense band at 962 cm^{-1} arises from the symmetric stretching modes and is designated as ν_1 fundamental vibrational mode. The bands comprising the fourth group arise from the ν_3 fundamental vibrational modes and are due to the asymmetric stretching vibrations of the P–O bonds these bands are seen at ~ 1025, 1047 and 1087 cm^{-1}.

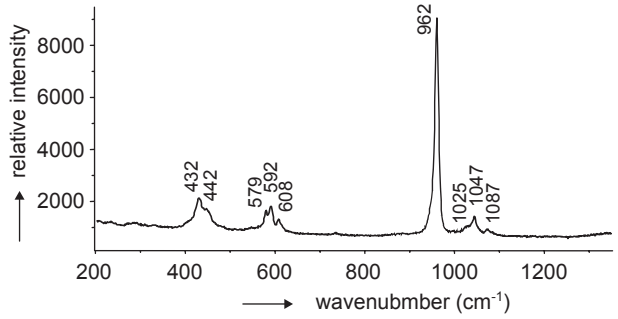

Figure 2. Raman spectrum of the monophasic hydroxyapatite.

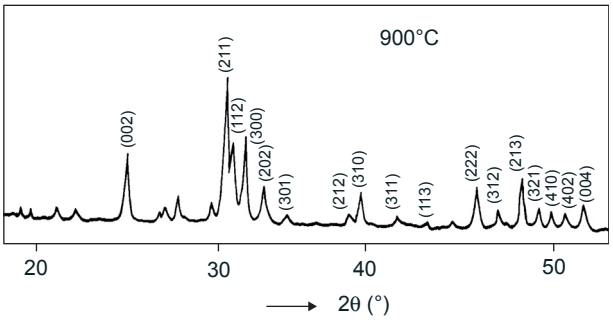

Figure 3. X-ray diffraction patterns of the monophasic hydroxyapatite.

X- ray diffraction analysis

Figure 3 shows the XRD patterns of HAP powder sintered at 900°C. The *d* spacings are compared with the JCPDS #74-0566 standard for HAP in table 1. It can be seen that there is a good agreement with the standard both in terms of intensity and position of the lines [14]. In addition to HAP patterns, no other diffraction pattern appears. It suggests that pure monophasic crystalline HAP phase can be produced at 900°C. The degree of crystallinity influences the dissolution and the biological behavior of HAP. Recent studies have shown that more crystalline structure induced lesser dissolution of the HAP [15].

It can be interpreted by the discussion that sharp reflection peak appears in the range of 31.8-52.5° 2θ representing the characteristic peak of apatite phase (JCPDS file no 9-432). Some characteristic peaks, for instance at (002), (112), (300), and (211) planes were observed for powder annealed at 900°C suggesting that the apatite powder with structural evolution from amorphous to crystalline were possible depending on the annealing temperatures. The patterns demonstrate the stable nature of HAP with no extraneous peaks, indicating the presence of stoichiometric HAP with Ca/P ratio of 1.67 after sintering.

STEM and X-ray micro analysis

The STEM image of HAP showed mill-fractured surface of a HAP particle, where the EDXS (figure 4) detected Ca, P, O, Cl and Cu, among which the Cu was revealed by grid supporting and Cl from the polymer film. The elemental composition, i.e. Ca, P and O content HAP, was studied by EDXS for each analysis an EELS spectrum acquired in the low loss region to obtain the local relative thickness in order to perform the quantitative analysis. The analysis found the Ca/P atomic

Table 1. Plane spacings and intensities obtained from XRD.

d (nm) experimental	JCPDS	intensity experimental	JCPDS	(hkl)
0.3445	0.3440	33	40	002
0.2812	0.2814	100	100	211
0.2774	0.2778	48	60	112
0.2719	0.2720	62	60	300
0.2632	0.2631	22	25	202
0.2292	0.2295	9	8	212
0.2261	0.2262	23	20	310
0.2144	0.2148	7	10	311
0.1944	0.1943	36	30	222
0.1891	0.1890	17	16	312
0.1841	0.1841	41	40	213
0.1802	0.1806	19	20	321
0.1788	0.1780	15	12	410
0.1753	0.1754	20	16	402
0.1722	0.1722	19	20	004

ratio of the specimen was exactly 1.67, as was expected by stoichiometric composition of HAP ($Ca_{10}(PO_4)_6(OH)_2$). Figure 5 shows the morphologies of the HAP powder. The HAP samples showed nano-structured ellipse-like morphology. However, the powders sintered at 900°C with prolonged aging shows well dispersed particles. It suggests that the long ageing time favors the formation of large crystals than those aged for short duration of time. Ageing plays a crucial role in the formation of well crystallised hydroxyapatite particles.

CONCLUSION

Monophasic HAP bioceramic was synthesized using $Ca(NO_3)_2{\cdot}4H_2O$ and triethyl phosphite by simple sol-gel approach. FT-IR, Raman, XRD and STEM results suggests the presence of phase pure crystalline HAP particle after calcination at 900°C. The degree of crystallinity and morphology of the resulting powders are mainly depends on the processing parameters. The ability to generate crystalline HAP combined with the low processing temperature renders the sol-gel approach favorable for generating HAP coatings on various metallic substrates for biomedical applications.

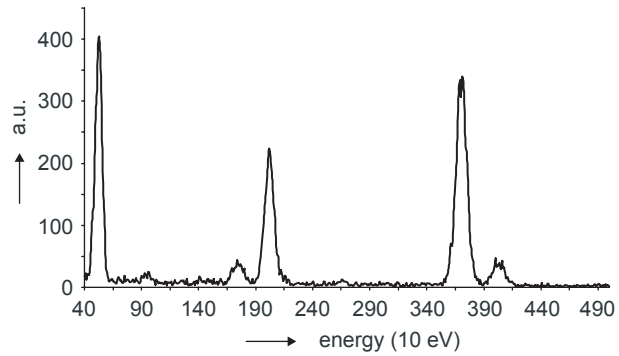

Figure 4. Energy dipersive X-ray electron microscopy analysis of monophasic HAP.

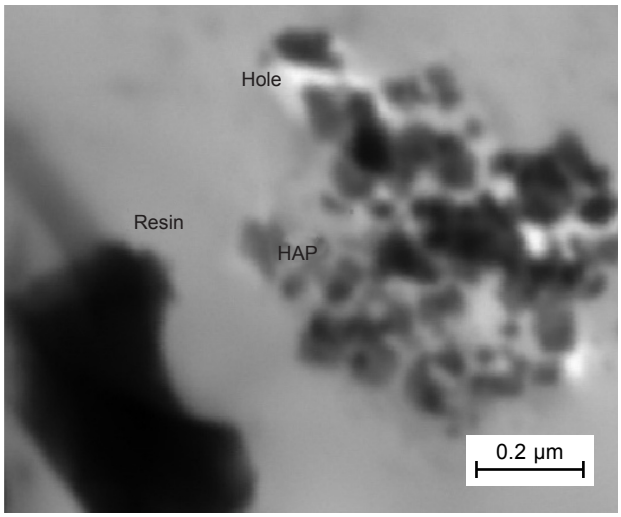

Figure 5. STEM micrograph of the monophasic hydroxyapatite.

Acknowledgement

The authors are gratefully acknowledge the financial support of the Université de Reims and Region Champagne-Ardenne, France.

References

1. Cheng K., Weng W., Han G., Du. P., Shen G., Yang J., Ferreira J. M. F.: J.Mater.Chem.Phys. *78*, 159 (2003).
2. Riman R. E., Suchanek W. L., Byraopa K., Chen C. W., Shuk P., Oakes C. S.: Solid State Ionics *151*, 89 (2002)
3. Weng W., Zhang S., Cheng K., Qu H., Du P., Shen G., Yuan J., Han G.: Surf.Coat.Tech. *167*, 54 (2003).
4. Jillavenkatesa A., Condrate R.A.: J.Mater.Sci. *33*, 411 (1998).
5. Balamurugan A., Kannan S., Rajeswari S.: Can.Met. Quart. *43*, 3 (2004).
6. Liu D. M., Chou H. M., Wu J. D.: J.Mater.Sci.Mater. Med. *5*, 1721 (1994).
7. Cliff G., Lorimer G. W.: J.Micro. *103*, 203 (1975).
8. Bauchet V., Michel J., Jallot E., Laurent-Maquin D., Balossier G.: J.Phys.D.Appl.Phys *36*, 1599 (2003).
9. Gross K. A., Phillips M.: J.Mater.Sci.Mater.Med. *9*, 797 (1998).
10. Livage J., Barboux P., Taulelle F.: J.Non-Cryst.Solids *147/148*, 211 (1992).
11. Van der Houwen J. A. M., Cressey G., Cressy B. A., Valsami-Jones E.: J.Cryst.Growth *249*, 96 (2003).
12. Rapacz-Kmita A., Elósarczyk A., Paszkiewicz Z. C., Paluszkiewicz C.: J.Mol.Struct. *704*, 65 (2004).
13. Smeulders D. E., Wilson M. A., Armstrong L.: Ind.Eng. Chem.Res. *40*, 10 (2001).
14. Toth J. M., Hirthe W. M., Hubard W. G., Brantley W. A., Lynch K. L.: J.Appl.Biomat. *2*, 169 (1991).
15. Sun L., Berndt C. C., Grey C. P.: Mater.Sci.Eng. A *360*, 135 (2003).

SYNTÉZA STECHIOMETRICKÉHO MONOFÁZOVÉHO HYDROXYAPATITU A JEHO STRUKTURNÍ ANALÝZA

A. BALAMURUGAN, J. MICHEL, J. FAURÉ, H.B ENHAYOUNE, L. WORTHAM, G. SOCKALINGUM*, V. BANCHET**, S. BOUTHORS**, D. LAURENT-MAQUIN*, G. BALOSSIER

INSERM ERM 0203, Laboratoire de Microscopie Electronique Analytique, Université de Reims
**Unité MéDIAN, CNRS UMR 6142, UFR de Pharmacie, Université de Reims*
***Laboratoire de Tribologie et de Dynamique des Surfaces (LTDS), UMR CNRS 5513, Ecole Centrale de Lyon*

Tento článek referuje o nové sol-gel technice přípravy prášku monofázového hydroxyapaptitu (HAP) $Ca_{10}(PO_4)_6(OH)_2$. Jako prekurzory fosforu a vápníku byly použity trietyl fosforitan a dusičnan vápenatý při stechimometrickém poměru Ca/P 1,67. Získané prášky byly vysušeny a kalcinovány při teplotách do 900 C. Rtg prášková difrakční analýza a Ramanova spektra ukázala přítomnost fázově čistého HAP. Prášky také vykazovaly charakteristický pík HAP v infračerveném spektru. Morfologická charakterizace HAP prášků byla provedená metodami STEM, EDXS a EELS. STEM mikrosnimky indikují povrch HAP částic morfologicky srovnatelný s mletým práškem. Elementární složení analyzované EDXS a EELS ukázalo, že prášek kalcinovaný při 900°C obsahuje monofázový stechiometrický HAP.